Thermal Control Compensation of Induction Motor Drive in Electrified Powertrain

S. M. Nawazish Ali*, Student member, IEEE, M. J. Hossain†, Senior member, IEEE, Vivek Sharma*, Student member, IEEE and Muhammad Kashif*
Student member, IEEE
*School of Engineering Macquarie University, Australia
Email: syed-muhammad-nawazish.ali@hdr.mq.edu.au
†School of Electrical and Data Engineering, University of Technology Sydney, Ultimo, NSW-2007, Australia
Email: jahangir.hossain@uts.edu.au

***Abstract*—The increase in operating as well as environmental temperature of an electric vehicle (EV) motor drive causes significant variations in its performance parameters such as rotor, stator resistance and mutual inductance. This variation results in the overall performance degradation of electrified powertrain in the form of excessive fuel (battery) consumption and inability to meet the desired terminal characteristics such as speed, torque and flux. To mitigate this issue, a robust linear parameter varying (LPV) control incorporated with linear matrix inequalities (LMIs) is presented in this work that ensures L_2 gain bound and closed-loop control system stability. A comparison of sliding mode control (SMC) is made with the proposed controller to validate its robustness. In order to verify the efficacy of LPV controller, its performance is tested against a New European Driving Cycle (NEDC) in MATLAB Simulink environment. The nonlinear simulation results gurantee the excellence of LPV performance.**

***Index Terms*—Induction Motor Drive; Parameter Uncertainities; LPV Control Technique; Electrified Powertrain; Linear Matrix Inequalities.**

I. Introduction

The environmental threats such as global warming, excessive greenhouse gas emissions and energy resource constraints have resulted in a world energy crisis. Transportation sector is suffering from excessive oil consumption due to ever increasing use of combustion engine based vehicles. Electric vehicles provide an ideal solution to cater these environmental and economical challenges [1]. However, the performance capability of their electrified powertrain is affected during vehicle operation due to signficant temperature rise.

Since the combustion engine is replaced by an electric motor in EVs, it is considered as the most important component while addressing the energy consumption and performance efficieny. Induction motors have been used in electrified powertrains such as in that of Tesla Roadster because of low maintenance feature and its de-excited nature against inverter fault [2]. Some other examples of electric and hybrid electric vehicles using induction motor are BMW/X5 (Germany), Toyota RAV4 and HondaFit EV (2012) [3]. During vehicle operation, the induction motor experiences parameter uncertainities due to temperature, road load and traffic conditions that cause degradation in the performance of electrified powertrain resulting in excessive battery consumption. Even a slight increase of 10°C beyond the motor's thermal limit reduces the stator insulation life by half [4]. The motor peformance is improved either by altering its physical design or by using closed-loop controllers. To meet the robustness and design objectives, various control techniques have been implemented to achieve performance optimization [5].

SMC approach is adopted in [6] for the parameters uncertainity issue in hybrid and pure electric vehicles but this control technique experiences chattering issue due to which it is difficult to achieve performance optimization of electrified powertrain. Although, higher order SMC is presented in [7] to address this issue but its implementation is quite complex. On the other hand, LPV control is implemented by some researchers to resolve problems in various applications of induction motor drive by considering the inherent dynamics of plant [8].

An LPV controlled induction motor setup is presented in [9] but it only considers the variation in rotor resistance. Load torque and rotor resistance uncertainities are controlled through LPV technique in [10]. An induction motor control design via quasi LPV approach is given in [11]. An LPV framework for induction machine is discussed in [12] but it only considers the shaft angle uncertainity. An LPV controller design with only 20% uncertainity in induction motor's rotor resistance is achieved in [13]. The variation of rotor resistance and frequency in an induction motor is controlled with LPV control in [14]. Authors have reported the LPV control approach for the change in rotor and stator resistances individually to address the deterioration in dynamic characteristics of three phase induction motor [15], [16]. The mentioned research works are not in the context of EVs. Moreover, they do not consider the simultaneous variations of rotor, stator resistance and mutual inductance. The variation of these parameters with drive temperature has significant impact in the drive energy consumption and performance capability of electrified powertrain. For this purpose, an output feedback based LPV observer and controller design is proposed in this research with EV as application. As per the standard for evaluation by the automotive community [17], the proposed control technique is validated against NEDC (a standard driving cycle).

The rest of the paper is organized as follows: Section II presents the mathematical modelling of induction motor and electric vehicle. The LPV observer and controller design synthesis is discussed in Section III. Section IV describes the performance evaluation of the proposed control technique. Section V presents the concluding remarks.

II. Induction Motor and EV Dynamics

A. Modelling of Induction Motor

A nonlinear bench mark mathematical model of induction motor in stationary frame of reference $\alpha-\beta$ axis is given by [15]:

$$\begin{aligned}\dot{\omega}_r &= \rho_0(\psi_{\alpha r}i_{\beta s} - \psi_{\beta r}i_{\alpha s}) - (\rho_7 B\omega_r) - (\rho_7\tau_L)\\ \dot{i}_{\alpha s} &= -\rho_1 i_{\alpha s} + \rho_2\psi_{\alpha r} + \rho_3\psi_{\beta r} + \rho_4 V_{\alpha s}^2\\ \dot{i}_{\beta s} &= -\rho_1 i_{\beta s} + \rho_2\psi_{\beta r} - \rho_3\psi_{\alpha r} + \rho_4 V_{\beta s}^2\\ \dot{\psi}_{\alpha r} &= -\rho_5\psi_{\alpha r} - n_p\omega_r\psi_{\beta r} + \rho_6 i_{\alpha s}\\ \dot{\psi}_{\beta r} &= -\rho_5\psi_{\beta r} + n_p\omega_r\psi_{\alpha r} + \rho_6 i_{\beta s}\end{aligned} \quad (1)$$

where $\rho_0=\frac{n_pL_m}{JL_r}$, $\rho_1=\frac{(L_m^2R_r+L_r^2R_s)}{\sigma L_sL_r^2}$, $\rho_2=\frac{L_mR_r}{\sigma L_sL_r^2}$, $\rho_3=n_p\frac{L_m\omega_R}{\sigma L_sL_r}$, $\rho_4=\frac{1}{\sigma L_s}$, $\rho_5=\frac{R_r}{L_r}$, $\rho_6=\frac{L_mR_r}{L_r}$, $\rho_7=\frac{1}{J}$, $\sigma = 1-\frac{L_m^2}{L_sL_r}$, ω_r is the angular velocity of motor, $i_{\alpha s}$ and $i_{\beta s}$ are the $\alpha-\beta$ stator currents, $\psi_{\alpha r}$ and $\psi_{\beta r}$ are the $\alpha-\beta$ rotor fluxes, $V_{\alpha s}$ and $V_{\beta s}$ represent the stator voltages.

The torque, speed and flux of induction motor is given by:

$$\tau_e = \zeta(\psi_{\alpha r}i_{\beta s} - \psi_{\beta r}i_{\alpha s}) \quad (2)$$

$$\omega_r = \int \frac{\zeta}{J}(\psi_{\alpha r}i_{\beta s} - \psi_{\beta r}i_{\alpha s}) - (\frac{B}{J}\omega_r) - (\frac{1}{J}\tau_L) \quad (3)$$

$$\psi_r = \sqrt{\psi_{\alpha r}^2 + \psi_{\beta r}^2} \quad (4)$$

where $\zeta=\frac{3}{2}\frac{n_pL_m}{L_r}$ and τ_L represents the load torque.

B. Dynamics of Electric Vehicle

For EV, the traction force is given by [18]:

$$F_t = F_r + F_i + F_g + F_a \quad (5)$$

where these forces are categorized as:
F_r : rolling resistance
F_i : inertial resistance
F_g : grade resistance
F_a : aerodynamic drag

The speed of EV ($n_{veh.}$) proportional to the speed of induction motor (ω_r) is given by:

$$n_{veh.} = \frac{R_w}{G}\omega_r \quad (6)$$

where G is the EV gair ratio and R_w is the EV wheel radius. The load torque ($\tau_{Lveh.}$) for EV is given by:

$$\tau_{(Lveh.)} = \frac{R_wF_t}{G} \quad (7)$$

C. Dynamics of Induction Motor in LPV framework

The transformation of induction motor nonlinear model (1) into an LPV framework model is made by taking R_r, R_s and L_m as the varying parameter with respect to time. The state space form of this model is given by:

$$\begin{aligned}\mathbf{G}(\boldsymbol{\delta(t)}) : \dot{\boldsymbol{x}} &= \boldsymbol{A(\delta(t))x} + \boldsymbol{B(\delta(t))u}\\ \mathbf{y} &= \boldsymbol{C(\delta(t))x} + \boldsymbol{D(\delta(t))u}\end{aligned} \quad (8)$$

where $\boldsymbol{\delta(t)}=[\delta_1\ \delta_2\ \delta_3]^T=[\ R_r(t)\ R_s(t)\ L_m(t)]^T$ is the time varying parameter, $\boldsymbol{u(t)}=[V_{\alpha s}\ V_{\beta s}]^T$, $\boldsymbol{y(t)}=[i_{\alpha s}\ i_{\beta s}]^T$ and $\boldsymbol{x(t)}=[i_{\alpha s}\ i_{\beta s}\ \psi_{\alpha r}\ \psi_{\beta r}]^T$. The system matrix for LPV framework of induction motor model is given as follows:

$$\mathbf{A}(\boldsymbol{\delta(t)}) = \begin{bmatrix} -(\frac{\delta_2}{\chi}+\frac{\delta_1\delta_3^1}{\chi L_r^2}) & 0 & \frac{\delta_1\delta_3}{\chi L_r^2} & \frac{n_p\omega_r\delta_3}{\chi L_r}\\ 0 & -(\frac{\delta_2}{\chi}+\frac{\delta_1\delta_3^1}{\chi L_r^2}) & -\frac{n_p\omega_r\delta_3}{\chi L_r} & \frac{\delta_1\delta_3}{\chi L_r^2}\\ \frac{\delta_1\delta_3}{L_r} & 0 & -\frac{\delta_1}{L_r} & -n_p\omega_r\\ 0 & \frac{\delta_1\delta_3}{L_r} & n_p\omega_r & -\frac{\delta_1}{L_r}\end{bmatrix}$$

$$\mathbf{B} = \begin{bmatrix}\frac{1}{\chi} & 0\\ 0 & \frac{1}{\chi}\\ 0 & 0\\ 0 & 0\end{bmatrix}, \mathbf{C} = \begin{bmatrix}1 & 0 & 0 & 0\\ 0 & 1 & 0 & 0\end{bmatrix}, \mathbf{D} = \begin{bmatrix}0 & 0\\ 0 & 0\end{bmatrix} \quad (9)$$

where $\chi=\sigma L_s$, **D**, **C** (output matrix) and **B** (input matrix) are fixed matrices.

III. Synthesis of Observer and Controller in LPV Framework

The closed-loop inner current control using LPV observer and controller is shown in the dotted section of Fig. 1. Its subsections are classified below:

A. Synthesis of LPV Observer

Unlike the industrial applications, motor flux in vehicles is continuously varying as per the driving cycle conditions, traffic situations and temperature. Its variation directly affects the terminal characteristics of motor as well as the drive energy consumption [19]. Hence, it is necessary to accurately estimate these flux variations caused by parameters (rotor, stator and mutual inductance) uncertainities and also their effect on the vehicular speed. For this purpose, an LPV observer is synthesized which estimates the angular velocity through flux estimation. The observer is given as follows:

$$\begin{bmatrix}\dot{\hat{\mathbf{i}}}_{\mathbf{S}}^{\mathbf{s}}\\ \dot{\hat{\boldsymbol{\psi}}}_{\mathbf{r}}^{\mathbf{s}}\end{bmatrix} = \begin{bmatrix}\mathbf{A_{11}}(\delta) & \mathbf{A_{12}}(\delta)\\ \mathbf{A_{21}}(\delta) & \mathbf{A_{22}}(\delta)\end{bmatrix}\begin{bmatrix}\hat{\mathbf{i}}_{\mathbf{S}}^{\mathbf{s}}\\ \hat{\boldsymbol{\psi}}_{\mathbf{r}}^{\mathbf{s}}\end{bmatrix} + \mathbf{B}\mathbf{V}_{\mathbf{S}}^{\mathbf{s}} + \mathbf{L}(\delta)\left\{\mathbf{i}_{\mathbf{S}}^{\mathbf{s}} - \mathbf{C}\begin{bmatrix}\hat{\mathbf{i}}_{\mathbf{S}}^{\mathbf{s}}\\ \hat{\boldsymbol{\psi}}_{\mathbf{r}}^{\mathbf{s}}\end{bmatrix}\right\} \quad (10)$$

where $\boldsymbol{V_S^s}=[V_{\alpha s}\ \ V_{\beta s}]^T$, $\boldsymbol{L(\delta)}$ is the gain matrix, $\boldsymbol{i_S^s}=[i_{\alpha s}\ i_{\beta s}]^T$ and $\boldsymbol{\psi_r^s}=[\psi_{\alpha r}\ \psi_{\beta r}]^T$. The estimated angular velocity is given by:

$$\hat{\omega}_r = \frac{\zeta}{J}(\hat{\psi}_{\alpha r}i_{\beta s} - \hat{\psi}_{\beta r}i_{\alpha s}) - (\frac{B}{J}\hat{\omega}_r) - (\frac{1}{J}\tau_L) \quad (11)$$

$$\mathbf{A_{11}} = \begin{bmatrix}-\frac{(L_m^2R_r+L_r^2R_s)}{\sigma L_sL_r^2} & 0\\ 0 & -\frac{(L_m^2R_r+L_r^2R_s)}{\sigma L_sL_r^2}\end{bmatrix}$$

$$\mathbf{A_{12}} = \begin{bmatrix}\frac{L_mR_r}{\sigma L_sL_r^2} & n_p\omega_r\frac{L_m}{\sigma L_sL_r^2}\\ -n_p\omega_r\frac{L_m}{\sigma L_sL_r^2} & \frac{L_mR_r}{\sigma L_sL_r^2}\end{bmatrix}$$

$$\mathbf{A_{21}} = \begin{bmatrix}\frac{L_mR_r}{L_r} & 0\\ 0 & \frac{L_mR_r}{L_r}\end{bmatrix}, \mathbf{A_{22}} = \begin{bmatrix}-\frac{R_r}{L_r} & -n_p\omega_r\\ n_p\omega_r & -\frac{R_r}{L_r}\end{bmatrix} \quad (12)$$

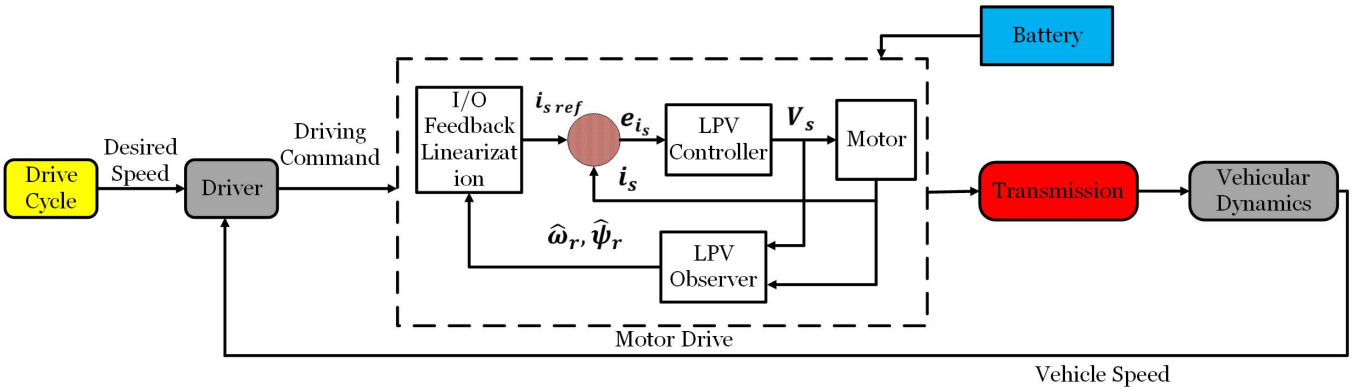

Fig. 1: Electric vehicle simulator

B. Synthesis of LPV Controller

The reference stator currents are tracked even in the presence of varying parameters by using LPV controller for the motor model (9). LPV controller design initiates with a generalized plant concept which is inherently an augmented plant and is given by:

$$\dot{\mathbf{x}}(t) = \boldsymbol{A}(\boldsymbol{\delta}(t))\boldsymbol{x}(t) + \boldsymbol{B_w}(\boldsymbol{\delta}(t))\boldsymbol{w}(t) + \boldsymbol{B_u}(\boldsymbol{\delta}(t))\boldsymbol{u}(t)$$
$$\boldsymbol{z}(t) = \boldsymbol{C_z}(\boldsymbol{\delta}(t))\boldsymbol{x}(t) + \boldsymbol{D_{zw}}(\boldsymbol{\delta}(t))\boldsymbol{w}(t) + \boldsymbol{D_{zu}}(\boldsymbol{\delta}(t))\boldsymbol{u}(t)$$
$$\boldsymbol{v}(t) = \boldsymbol{C_y}(\boldsymbol{\delta}(t))\boldsymbol{x}(t) + \boldsymbol{D_{yw}}(\boldsymbol{\delta}(t))\boldsymbol{w}(t) \quad (13)$$

where $\boldsymbol{z}$ is elaborated in [15], $\boldsymbol{y}$=$\boldsymbol{v}$=$[i_{\alpha s}\ i_{\beta s}]^T$ and $\boldsymbol{w}$ = $[i_{\alpha sref}\ i_{\beta sref}]^T$. $\boldsymbol{A}, \boldsymbol{B_w}, \boldsymbol{B_u}, \boldsymbol{C_z}, \boldsymbol{D_{zw}}, \boldsymbol{D_{zu}}, \boldsymbol{C_y}$ and $\boldsymbol{D_{yw}}$ are the LPV control system matrices. The variable parameter is δ which can be written as:

$$\boldsymbol{\delta(t)} = (\delta_1, \delta_2, ..., \delta_L)^T \quad (14)$$

The range of each δ_i is given as:

$$\delta_i(t)\ \epsilon\ [\delta_{min}\ \delta_{max}] \quad (15)$$

$\boldsymbol{A(\delta(t))}$ in its expanded form is given as:

$$\boldsymbol{A(\delta(t))} = \boldsymbol{A_0} + \boldsymbol{R_r A_1} + \boldsymbol{R_s A_2} + \boldsymbol{L_m A_3} \quad (16)$$

The convex decomposition for $\boldsymbol{\delta(t)}$ is given by:

$$\delta(t) \quad = \quad \alpha_1\delta_1 + \alpha_2\delta_2 + \alpha_3\delta_3 + ... + \alpha_8\delta_8 \quad (17)$$

with

$$\sum_{i=1}^{8} \alpha_i = 1\ and\ \alpha_i \geq 0$$

The polytopic induction motor plant incorporating the vertices of δ is given by:

$$\mathbf{G}(\delta) \quad = \quad \alpha_1\mathbf{G}(\delta_1) + \alpha_2\mathbf{G}(\delta_2) + \alpha_3\mathbf{G}(\delta_3) + ... + \alpha_8\mathbf{G}(\delta_8) \quad (18)$$

LPV controller in its dynamic form is represented by:

$$\dot{\boldsymbol{x}}_K = \boldsymbol{A_K}(\boldsymbol{\delta(t)})\boldsymbol{x_K} + \boldsymbol{B_K}(\boldsymbol{\delta(t)})\boldsymbol{y}$$
$$\boldsymbol{u} = \boldsymbol{C_K}(\boldsymbol{\delta(t)})\boldsymbol{x_K} + \boldsymbol{D_K}(\boldsymbol{\delta(t)})\boldsymbol{y} \quad (19)$$

such that the L_2 norm which is bounded by $\gamma > 0$ and internal stability of the closed-loop system ((13) and (19)) are satisfied through mapping from $\boldsymbol{w}$ to $\boldsymbol{z}$. By solving the LMIs given below [20], $\boldsymbol{A_K}$, $\boldsymbol{B_K}$, $\boldsymbol{C_K}$ and $\boldsymbol{D_K}$ (controller matrices) are calculated. The optimal value for γ is ensured by these LMIs.

$$\begin{bmatrix} \mathbf{AN} + \mathbf{NA}^T + \mathbf{B_u}\tilde{\mathbf{C}}_\mathbf{K} + (\mathbf{B_u}\tilde{\mathbf{C}}_\mathbf{K})^T & \tilde{\mathbf{A}}_\mathbf{K} + \mathbf{A} + \\ * & \mathbf{A}^\mathbf{T}\mathbf{M} + \mathbf{MA} + \\ * & * \\ * & * \\ \mathbf{B_u}\tilde{\mathbf{D}}_\mathbf{K}\mathbf{C_y} & \mathbf{B_u} + \mathbf{B_u}\tilde{\mathbf{D}}_\mathbf{K}\mathbf{D_{yw}} \\ \tilde{\mathbf{B}}_\mathbf{K}\mathbf{C_y} + (\tilde{\mathbf{B}}_\mathbf{K}\mathbf{C_y})^T & \mathbf{MB_w} + \tilde{\mathbf{B}}_\mathbf{K}\mathbf{D_{yw}} \\ & -\gamma\mathbf{I} \\ & * \end{bmatrix}$$
$$\begin{bmatrix} (\mathbf{C_zN} + \mathbf{D_{zu}}\tilde{\mathbf{C}}_\mathbf{K})^T \\ (\mathbf{C_z} + \mathbf{D_{zu}}\tilde{\mathbf{D}}_\mathbf{K}\mathbf{C_y})^T \\ (\mathbf{D_{zw}} + \mathbf{D_{zu}}\tilde{\mathbf{D}}_\mathbf{K}\mathbf{D_{yw}})^T \\ -\gamma\mathbf{I} \end{bmatrix} < 0 \quad (20)$$

$$\begin{bmatrix} \mathbf{N} & \mathbf{I} \\ \mathbf{I} & \mathbf{M} \end{bmatrix} > 0 \quad (21)$$

The optimized value of γ comes out to be 0.8020. The controller matrices are calculated from the symmetric matrices $\mathbf{N}(\delta)$ and $\mathbf{M}(\delta)$ and the gain matrices $\widetilde{\mathbf{A}}_\mathbf{K}(\delta)$, $\widetilde{\mathbf{B}}_\mathbf{K}(\delta)$, $\widetilde{\mathbf{C}}_\mathbf{K}(\delta)$, $\widetilde{\mathbf{D}}_\mathbf{K}(\delta)$ by using the following equations:

$$\mathbf{D_K} = \tilde{\mathbf{D}}_\mathbf{K} \quad (22)$$

$$\mathbf{C_K} = (-\mathbf{D_K}\mathbf{C_y}\mathbf{N} + \tilde{\mathbf{C}}_\mathbf{K})(\mathbf{V}^T)^{-1} \quad (23)$$

$$\mathbf{B_K} = \mathbf{W}^{-1}(-\mathbf{MB_u}\mathbf{D_K} + \tilde{\mathbf{B}}_\mathbf{K}) \quad (24)$$

$$\mathbf{A_K} = \mathbf{W}^{-1}(\tilde{\mathbf{A}}_\mathbf{K} - \mathbf{WB_K}\mathbf{C_y}\mathbf{N} - \mathbf{MB_u}\mathbf{C_K}\mathbf{V}^T - \mathbf{M}(\mathbf{B_u}\mathbf{D_K}\mathbf{C_y} + \mathbf{A})\mathbf{N})(\mathbf{W}^T)^{-1} \quad (25)$$

where the matrices $\mathbf{V}$ and $\mathbf{W}$ are used as follows:

$$\mathbf{I} - \mathbf{MN} = \mathbf{WV}^T \quad (26)$$

Hence, LPV control structure in polytopic representation is given as:

$$\begin{bmatrix} \mathbf{A_K}(\delta) & \mathbf{B_K}(\delta) \\ \mathbf{C_K}(\delta) & \mathbf{D_K}(\delta) \end{bmatrix} = \sum_{i=1}^{8} \alpha_i \begin{bmatrix} \mathbf{A_K}(\delta_i) & \mathbf{B_K}(\delta_i) \\ \mathbf{C_K}(\delta_i) & \mathbf{D_K}(\delta_i) \end{bmatrix} \quad (27)$$

TABLE I: Model Specifications

Vehicle Specifications		
Parameter	Symbol	Value
Mass	m	1000 kg
Wheel radius	R_w	0.2 m
Coefficient of rolling resistance	C_r	0.014
Frontal area	A_f	2.1 m^2
Coefficient of aerodynamic drag	C_d	0.4
Motor Specifications		
number of pole-pairs	n_p	2
stator self-inductance	L_s	0.0425 H
rotor self-inductance	L_r	0.043 H
stator resistance	R_s	0.22 Ω
rotor resistance	R_r	0.209 Ω
moment of inertia	J	0.124 $kg.m^2$
damping coefficient	B	0.01 $N.m.sec.rad^{-1}$
magnetizing inductance	L_m	0.04 H

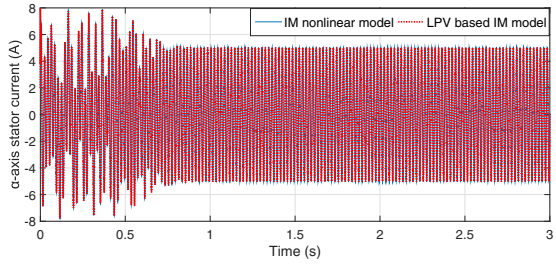

Fig. 2: $i_{\alpha s}$ state validation

C. Synthesis of Input Output Feedback Linearization (I/OFL)

The $\alpha - \beta$ axis stator reference currents are calculated through I/OFL technique applied on the motor's angular velocity and flux. The input and output vectors for I/OFL are $\mathbf{i_S^s} = [i_{\alpha s} \quad i_{\beta s}]^T$ and $\mathbf{y} = [\omega_r \quad \psi_r]^T$ respectively. IOFL yields the following stator reference currents that are used in motor drive.

$$i_{\alpha sref} = \frac{\hat{\psi}_{\alpha r}}{\kappa_3}\left(\frac{\dot{\hat{\psi}}_r}{\hat{\psi}_r} + \kappa_2\right) + \frac{\hat{\psi}_{\beta r}}{n_p \kappa_1 \kappa_4 \hat{\psi}_r^2}\left(-\dot{\hat{\omega}}_r - \kappa_4 \tau_L - \kappa_4 B \hat{\omega}_r\right) \tag{28}$$

$$i_{\beta sref} = \frac{\hat{\psi}_{\beta r}}{\kappa_3}\left(\frac{\dot{\hat{\psi}}_r}{\hat{\psi}_r} + \kappa_2\right) + \frac{\hat{\psi}_{\alpha r}}{n_p \kappa_1 \kappa_4 \hat{\psi}_r^2}\left(\dot{\hat{\omega}}_r + \kappa_4 \tau_L + \kappa_4 B \hat{\omega}_r\right) \tag{29}$$

where $\kappa_1 = \frac{n_p L_m}{J L_r}$, $\kappa_2 = \frac{R_r}{L_r}$, $\kappa_3 = \frac{L_m R_r}{L_r}$, $\kappa_4 = \frac{1}{J}$, $\dot{\hat{\psi}}_r$ is :

$$-\kappa_2 \hat{\psi}_r + \kappa_3 \frac{\hat{\psi}_{\alpha r} i_{\alpha s} + \hat{\psi}_{\beta r} i_{\beta s}}{\hat{\psi}_r} \tag{30}$$

and $\dot{\hat{\omega}}_r$ is calculated by taking the derivative of (11).

IV. Performance Validation of LPV

The performance of LPV control technique is validated through simulations of traction (induction) motor drive in EV framework. The model specifications of EV and motor given in Table I.

A. Model validation of LPV controller

The states of designed LPV model (9) which incorporates the variation of R_r, R_s and L_m are compared with those of induction motor nonlinear model (1). For the model accuracy validation, one state $i_{\alpha s}$ is plotted here in Fig. 2.

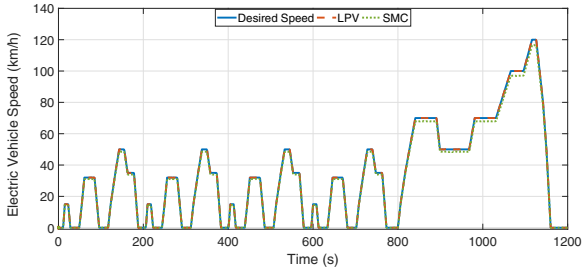

Fig. 3: NEDC analysis for LPV and SMC at 45°C

TABLE II: Comparison of SMC and LPV

Error	SMC	LPV
RMSE	0.2321	0.1472
NRMSE	0.8992	0.7968

B. NEDC based Driving Cycle Analysis

A vehicle simulator given in Fig. 1 is designed for testing the controller in MATLAB. The drive cycle (NEDC) is fed into the driver (proportional-integral control) block which generates the driving commands (acceleration and brake position). These commands are given to the motor drive block in which a combination of LPV controller and observer is responsible for current and speed control. The drive is powered by a battery. The drive output is given to vehicular dynamics through transmission. The vehicle speed is fedback to the driver block to form a closed-loop control architecture. The vehicular energy consumption increases by the increase in drive parameters (R_r, R_s and L_m) due to temperature rise which ultimately degrades its efficiency. For the performance validation of LPV at a high temperature of 45°C, it is analyzed using NEDC and also by comparing it with a first order SMC using the same vehicle simulator at the same conditions. The temperature variations are incorporated by relating them to those of resistances as follows [21]:

$$R = R_0[1 + \alpha \Delta T] \tag{31}$$

where R_0 corresponds to the reference temperature resistance, ΔT represents the temperature difference and α gives the resistance temperature coefficient. It can be inferred from Fig. 3 that LPV controller shows excellent tracking even at high temperatures in comparison to its control counterpart. Based on this result, a performance comparison of LPV and SMC is given in Table II.

C. NEDC Based Drive Flux

One of the adverse effects of Lm variation is the drive flux deterioration as given by [15]:

$$\psi_r = L_m i_{\alpha s} \tag{32}$$

The tracking of induction motor flux shown in Fig. 4 validates the excellent performance of LPV even in harsh environment.

D. NEDC Based Drive Energy Consumption

Since the supply voltage in EV is limited by battery capacity and charging status, the designed control technique should optimize its usage to reduce the battery energy consumption and enhance the overall drive performance of EV.

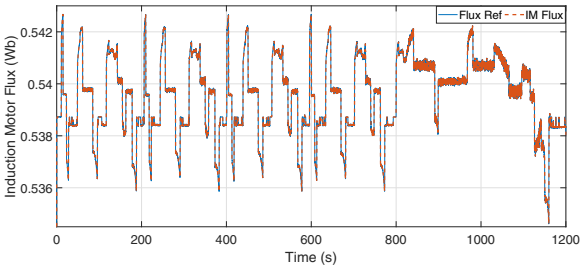

Fig. 4: NEDC based motor flux tracking

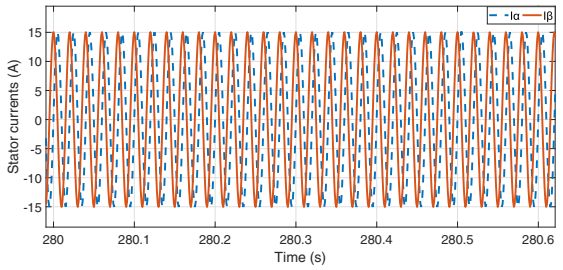

(a)

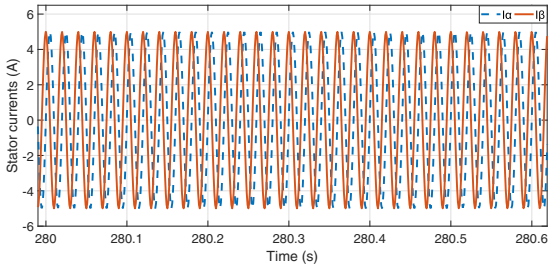

(b)

Fig. 5: Drive Currents: (a) SMC (b) LPV

For this purpose, the zoomed short-frame version of the currents and voltages obtained through LPV are compared with that of SMC against vehicle operation in NEDC at a high temperature of 45°C as shown in Figs. 5 and 6. The lesser consumption of voltage and current in case of LPV under thermally varying parameters proves its efficacy and robustness for the electrified powertrain.

E. Performance Improvement Analysis

The thermal effects in the developed MATLAB based simulator are considered through the parameters variation which are directly related to temperature changes as given by (31). The improved performance of LPV in comparison with SMC at a high temperature value is indicated through error values in vehicle speed tracking in Table II. Moreover, the improvement in voltage and current consumption at a high temperature is also highlighted through zoomed simulation results. It can be observed that for the given zoomed time interval, LPV technique based control voltages and currents are 138 V and 4.8 A in amplitude respectively which are less than SMC technique based control voltages and currents.

V. Conclusion

An LPV control technique is proposed to reduce the vehicle energy consumption in its electrified powertrain due

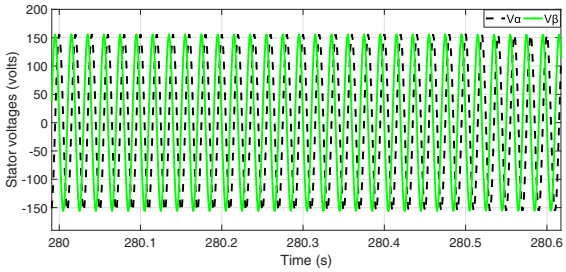

(a)

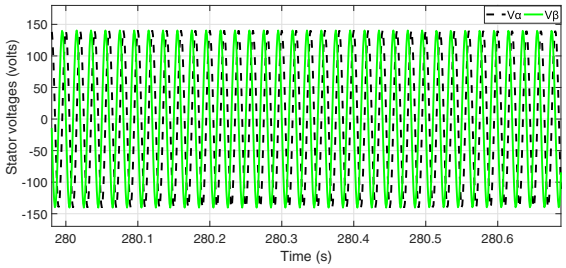

(b)

Fig. 6: Drive Voltages: (a) SMC (b) LPV

to the variation of drive parameters (rotor, stator resistance and mutual inductance) caused by the increase in operating and environmental temperature during vehicle operation. The robustness of the controller is tested against a standard driving cycle (NEDC). The efficacy of LPV and its improved performance against variations caused by thermal effects is ensured by comparing it with SMC. In future, interior permanent magnet synchronous motor will be studied in the light of thermal characteristics and LPV control.

References

[1] C. Chan, A. Bouscayrol, and K. Chen, "Electric, hybrid, and fuel-cell vehicles: Architectures and modeling," *IEEE Transactions on Vehicular Technology*, vol. 59, no. 2, 2010.

[2] S. N. Ali, J. Hossain, D. Wang, K. Lu, P. Rasmussen, V. Sharma, and M. Kashif, "Robust sensorless control against thermally degraded speed performance in an im drive based electric vehicle," *IEEE Transactions on Energy Conversion*, 2020.

[3] J. De Santiago, H. Bernhoff, B. Ekergård, S. Eriksson, S. Ferhatovic, R. Waters, and M. Leijon, "Electrical motor drivelines in commercial all-electric vehicles: A review," *IEEE Transactions on vehicular technology*, vol. 61, no. 2, pp. 475–484, 2011.

[4] W. Pawlus, J. T. Birkeland, H. Van Khang, and M. R. Hansen, "Identification and experimental validation of an induction motor thermal model for improved drivetrain design," *IEEE Transactions on Industry Applications*, vol. 53, no. 5, pp. 4288–4297, 2017.

[5] Z. Yang, F. Shang, I. P. Brown, and M. Krishnamurthy, "Comparative study of interior permanent magnet, induction, and switched reluctance motor drives for ev and hev applications," *IEEE Transactions on Transportation Electrification*, vol. 1, no. 3, pp. 245–254, 2015.

[6] R. De Castro, R. E. Araújo, and D. Freitas, "Wheel slip control of evs based on sliding mode technique with conditional integrators," *IEEE Transactions on Industrial Electronics*, vol. 60, no. 8, pp. 3256–3271, 2013.

[7] L. Zhao, J. Huang, H. Liu, B. Li, and W. Kong, "Second-order sliding-mode observer with online parameter identification for sensorless induction motor drives," *IEEE Transactions on Industrial Electronics*, vol. 61, no. 10, pp. 5280–5289, 2014.

[8] K. Zhou, J. C. Doyle, K. Glover *et al.*, *Robust and optimal control*. Prentice Hall New Jersey, 1996, vol. 40.

[9] A. Salem, A. S. Tlili, and N. B. Braiek, "On the polytopic and multimodel state observers of induction motors," *Journal of Automation and Systems Engineering (JASE)*, vol. 2, no. 4, pp. 235–247, 2008.

[10] E. Prempain, I. Postlethwaite, and A. Benchaib, "A linear parameter variant h∞ control design for an induction motor," *Control Engineering Practice*, vol. 10, no. 6, pp. 633–644, 2002.

[11] F. Farhani, C. B. Regaya, A. Zaafouri, and A. Chaari, "A quasi linear parameter varying approach to robust control of an induction machine," in *Systems, Signals & Devices (SSD), 2013 10th International Multi-Conference on*. IEEE, 2013, pp. 1–5.

[12] F. Blanchini, D. Casagrande, S. Miani, and U. Viaro, "An lpv control scheme for induction motors," in *Decision and Control (CDC), 2012 IEEE 51st Annual Conference on*. IEEE, 2012, pp. 7602–7607.

[13] K. Dalila, M. Abdessalem, D. Said, and L. Chrifi-Alaoui, "Robust linear parameter varying induction motor control with polytopic models," *Serbian Journal of Electrical Engineering*, vol. 10, no. 2, pp. 335–348, 2013.

[14] D. K. Abdessalem, D. Said *et al.*, "Linear parameter varying induction motor control with two-degree-of freedom controller," in *Power Engineering, Energy and Electrical Drives (POWERENG), 2013 Fourth International Conference on*. IEEE, 2013, pp. 1748–1752.

[15] S. N. Ali, A. Hanif, M. Hossain, and V. Sharma, "An lpv h∞ control design for the varying rotor resistance effects on the dynamic performance of induction motors," in *2018 IEEE 27th International Symposium on Industrial Electronics (ISIE)*. IEEE, 2018, pp. 114–119.

[16] S. N. Ali, M. Hossain, A. Hanif, V. Sharma, and M. Kashif, "A vrc h design for dynamic thermal derating of induction machines," in *2018 Australasian Universities Power Engineering Conference (AUPEC)*. IEEE, 2018, pp. 1–6.

[17] S. S. Williamson, A. Emadi, and K. Rajashekara, "Comprehensive efficiency modeling of electric traction motor drives for hybrid electric vehicle propulsion applications," *IEEE Transactions on Vehicular Technology*, vol. 56, no. 4, pp. 1561–1572, 2007.

[18] B. Tabbache, M. E. H. Benbouzid, A. Kheloui, and J.-M. Bourgeot, "Virtual-sensor-based maximum-likelihood voting approach for fault-tolerant control of electric vehicle powertrains," *IEEE Transactions on Vehicular Technology*, vol. 62, no. 3, pp. 1075–1083, 2013.

[19] S. Dilmi and S. Yurkovich, "Nonlinear torque control of the induction motor in hybrid electric vehicle applications," in *Proceedings of the 2005, American Control Conference, 2005.* IEEE, 2005, pp. 3001–3006.

[20] H. Werner, "Optimal and robust control-lecture notes," *Technical University Hamburg-Harburg, Institute of Control Engineering*, 2004.

[21] S. N. Ali, A. Hanif, and Q. Ahmed, "Review in thermal effects on the performance of electric motors," in *Intelligent Systems Engineering (ICISE), 2016 International Conference on*. IEEE, 2016, pp. 83–88.